Space Weather®

RESEARCH ARTICLE
10.1029/2021SW002902

Estimation of the Solar Wind Extreme Events

C. Larrodera[1], L. Nikitina[2], and C. Cid[1]

[1]Space Weather Research Group, Departamento de Física y Matemáticas, Universidad de Alcalá, Alcalá de Henares, Spain, [2]Canadian Hazards Information Service, Natural Resources Canada, Ottawa, ON, Canada

Key Points:

- Application of the extreme event analysis to the characteristic magnitudes of the solar wind
- Estimation of 1-in-40 and 1-in-80 years extreme values of different solar wind magnitudes
- Analysis of the Fréchet, Gumbel, and Weibull distribution function for estimation of extremes in the solar wind

Correspondence to:

C. Larrodera,
carlos.larrodera@edu.uah.es

Citation:

Larrodera, C., Nikitina, L., & Cid, C. (2021). Estimation of the solar wind extreme events. *Space Weather*, *19*, e2021SW002902. https://doi.org/10.1029/2021SW002902

Received 6 SEP 2021
Accepted 17 NOV 2021

Abstract This research provides an analysis of extreme events in the solar wind and in the magnetosphere due to disturbances of the solar wind. Extreme value theory has been applied to a 20-year data set from the Advanced Composition Explorer spacecraft for the period 1998–2017. The solar proton speed, solar proton temperature, solar proton density, and magnetic field have been analyzed to characterize extreme events in the solar wind. The solar wind electric field, vB_z has been analyzed to characterize the impact from extreme disturbances in the solar wind to the magnetosphere. These extreme values were estimated for 1-in-40- and 1-in-80-year events, which represent two and four times the range of the original data set. The estimated values were verified in comparison with measured values of extreme events recorded in previous years. Finally, our research also suggests the presence of an upper boundary in the magnitudes under study.

Plain Language Summary Space weather events are critical to modern technological infrastructure, and estimation of extreme space weather events is crucial for understanding potential the mitigation of risks associated with space weather hazards. This work is based on the analysis of extreme disturbances in the solar wind, which impacts the magnetosphere during space weather events. With use of data from the last 20 years, the largest events were analyzed, and with use of statistical approach, the maximum values expected for 1-in-40 and 1-in-80 years were estimated.

1. Introduction

Scientific progression in the last decades has made modern society more dependent on technology. Due to the interdependence between different components of technological infrastructure, a severe space weather event could cause a cascading effect in different aspects of modern life, from disruption in electric power grids to spacecraft malfunction and navigation problems. For example, one of the largest magnetic storms of the last century, occurring in March 1989, caused widespread effects in the Hydro-Québec power system in Canada (see e.g., Boteler, 2019). Riley et al. (2018) state that the cost of a worst-case scenario 1-in-100 years magnetic storm would include: (a) 1–2 Trillion USD dollars of economic loss; and (b) 130 million people without electrical power for several years, based on the destruction of several hundred transformers.

The main driver of geomagnetic storms is the solar wind; hence, knowledge of the most severe disturbances in the solar wind is essential to both forecast and to potentially mitigate risks related to space weather events. Extreme value theory (EVT) is a statistical method developed to analyze the likelihood of occurrence of rare and severe events (see Coles, 2001; Gumbel, 1958 and references therein). This theory has been applied in different fields, from hydrology and meteorology (see e.g., Gumbel, 1958) to finance (Embrechts & Schmidli, 1994) and public health (Thomas et al., 2016). In recent decades, EVT has been applied to estimate extreme values in different aspects of solar physics and space weather. In particular, extreme value analysis has been applied to the study of extreme geomagnetic storms (Chen et al., 2019; Elvidge, 2020; Love, 2019; Love et al., 2015; Nikitina et al., 2016; Siscoe, 1976; Thomson et al., 2011), solar energetic proton flux (Koons, 2001; Ruzmaikin et al., 2011), the electron flux in the outer belt of the magnetosphere (O'Brien et al., 2007), and to the analysis of the solar cycle (Acero et al., 2018; Asensio Ramos, 2018).

In the present study, EVT is applied to estimate extreme values of solar wind characteristics, such as the interplanetary magnetic field magnitude, the solar proton speed, the solar proton temperature, and solar proton density along with other magnitudes like the solar wind electric field, vB_z, to characterize the response of the magnetosphere to the extreme events in the solar wind. EVT also provides an opportunity to estimate the return value of these magnitudes, which is expected 1-in-40 and 1-in-80 years.

The paper is structured as follows: Section 2 details the statistical approach used in the analysis. Section 3 describes the data set and its temporal resolution. Section 4 shows EVT applied to different magnitudes of the solar wind. Finally, Section 5 shows the results and conclusions of the research.

2. Extreme Value Theory

Extreme value theory is a statistical method developed to analyze the likelihood of the occurrence of severe events, that is, events with a low probability of occurrence. For this analysis, the whole data set has been separated into blocks of the same duration, and then the EVT has been used to analyze the statistical behavior of the maximum values M_n for each block of data $X_1 \ldots X_n$, corresponding to a certain period of time (Coles, 2001).

$$M_n = \max(X_1, X_2, \ldots X_n), \tag{1}$$

where M_n are assumed to be independent and identically distributed.

The distribution of the maximum values (M_n) can be described by the generalized extreme value (GEV) distribution, which is defined by the cumulative probability (p) and depend on three parameters: the location parameter (μ), the scale parameter (σ), understood as the variance of the data, and the shape parameter (ξ), which defines the behavior of the tail of the GEV distribution. Depending on the sign of the shape parameter, the GEV distribution has three different forms:

(1) $\xi > 0 \Rightarrow$ Fréchet distribution,
(2) $\xi = 0 \Rightarrow$ Gumbel distribution,
(3) $\xi < 0 \Rightarrow$ Weibull distribution,

where the probability function for this distribution is:

$$p(M_n < z) = \exp\left(-\left[1 + \xi\left(\frac{z-\mu}{\sigma}\right)\right]^{-1/\xi}\right), \quad \text{if} \quad \xi \neq 0, \tag{2}$$

$$p(M_n < z) = \exp\left(-\exp\left(\frac{z-\mu}{\sigma}\right)\right), \quad \text{if} \quad \xi = 0. \tag{3}$$

Large disturbances in the solar wind produce severe space weather events that can last from hours to several days (Gopalswamy, 2016). Therefore, it is important to define the size of the blocks to capture the severe events and assure that they are independent. A block size of 2 days has been chosen for the extreme value analysis, checking that the M_n values are related to different space weather events. Extension of the block size to larger amount of days should provide approximately the same fitting results, but 2 days were chosen for the analysis to keep a larger data set and get more precise confidence intervals for extreme value estimation. Indeed, Zhang et al. (2008) estimate an average size of 41.2 hr for the ICMEs. In the case that two consecutive points have been selected, the lower one was discarded, assuring only one point per event.

To choose the proper distribution function (Fréchet, Gumbel, or Weibull) and perform a regression analysis, special coordinates that transfer the GEV distribution to a straight line were used. The coordinates for the regression analysis are the double logarithm of the probability $-\ln(-\ln(p))$ versus z for the case $\xi = 0$ (Equation 3) and the double logarithm $-\ln(-\ln(p))$ versus $\log(z)$ for the case $\xi \neq 0$ (Equation 2; Coles, 2001). The analyzed data set was fitted to both distributions (Equations 2 and 3) to obtain the shape parameter (ξ) from the fitting and the R-squared (R^2) to decide the appropriate distribution and proceed to further analysis.

The estimated return value (z) for a specific return period (T) can be calculated from the EVT using the probability $p(M_n < z)$:

$$T = \frac{1}{1 - p\ (M_n < z)}. \tag{4}$$

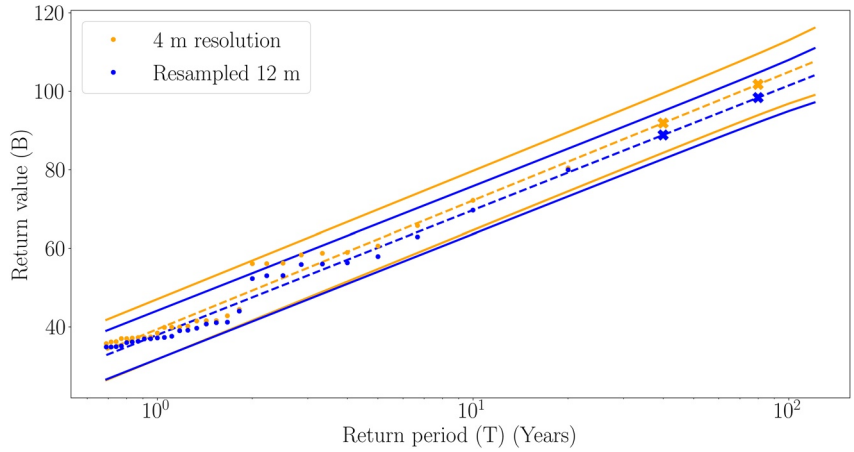

Figure 1. Fitting of the interplanetary magnetic field to an extreme value distribution for resampled 12 min resolution (blue line) and 4 min resolution (orange line) data. Crosses denote estimation for 1-in-40 and 1-in-80 year events, solid lines denote 99% confidence intervals.

3. Data Sample and Temporal Resolution

In this analysis, level 2 data from 1998 to 2017 from the Advanced Composition Explorer (ACE) spacecraft, which is located at the Lagrange point L1 were used. On one hand, the data set contains the solar proton speed (v) (with an energy range between 0.5 and 100 KeV), the solar proton density (N), the solar proton temperature (T) from the Solar Wind Electron Proton Alpha Monitor (SWEPAM/ACE; McComas et al., 1998), and the Solar Wind Ion Composition Spectrometer (SWICS/ACE; Gloeckler et al., 1998) with a temporal resolution of 12 min. On the other hand, the interplanetary magnetic field magnitude (B) and Z component (B_z) from the magnetometer (MAG; Smith et al., 1998) with a temporal resolution of 4 min were chosen. The MAG and SWEPAM instruments provide higher temporal resolutions, 1 and 16 s for MAG and 64 s for SWEPAM, but we decided to use 4 and 12 min temporal resolution, respectively, for this task. The data coverage is near 100% during the whole period of 20 years of analysis, which coincides with the first 20 years of life of the ACE mission, launched in August 1997. This 20-year period allows 1 to establish return periods that are two and four times the duration of the data set, that is, 1-in-40 and 1-in-80 years. To study the response of the magnetosphere to the disturbances created by the solar wind, the solar wind electric field ($E = v|B_z|$) has been analyzed. The largest values considered in our study has been set by the percentile 99 of the cumulative distribution function of each magnitude.

The use of data with different temporal resolutions can provide some effects in the results of the analysis (see e.g., Trichtchenko, 2021). Thus, the temporal resolution of B_z should be resampled to 12 min to match with the resolution of v. To study how the temporal resolution affects the results of the extreme value analysis for the solar wind, this analysis has been performed for one magnitude using two different temporal resolutions. Figure 1 shows the results of the EVT applied to the interplanetary magnetic field magnitude for different resolutions. The orange color is the 4-min data set from the instrument and the blue color is the resampled 12-min data set. The dots are the largest values for the analyzed 20-year data sets, while the straight lines represent 99% confidence interval linear fitting. The crosses are the estimations from the EVT for return values for 1-in-40- and 1-in-80-year events. As can be seen from the plot, the results are very similar. Indeed, the expected return values for 1-in-40 years are 92 and 89 nT, while for 1-in-80 years, the values are 102 and 98 nT for the 4 min resolution and resampled 12 min resolution, respectively. The difference between the results of the 4 and 12-min resolution data is less than 4% and can be neglected for this research.

4. Solar Wind Extreme Event Analysis

Extreme value theory was applied to the characteristic magnitudes of the solar wind: interplanetary magnetic field magnitude, solar proton speed, solar proton temperature, solar proton density, and solar wind electric field, vB_z. The temporal resolution of the used data set is 12 min, except for the interplanetary magnetic field magnitude, which is 4 min. As discussed in the previous section, 2 days block maximum values (M_n) were taken for the

Table 1
R-Squared (R^2) and Shape Parameter From the GEV Distribution Fit With a 99% Confidence Interval

		V	N	T	E	B
Gumbel distribution	R^2 ($\xi = 0$)	0.916	0.973	0.959	0.986	0.978
Fréchet distribution	R^2 ($\xi \neq 0$)	0.941	0.978	0.988	0.982	0.974
Shape parameter	ξ	0.52 ± 0.91	0.25 ± 0.31	0.53 ± 0.48	0.27 ± 0.33	0.31 ± 0.37

analysis. For consistency, higher resolution data, even when they are available, are not considered in this study. The probability function (p) was calculated based on the total number of blocks (N), and the position of each block (i) after rearranging M_i in ascending order, $p = i/N$.

To define which form of the extreme value distribution (Fréchet, Gumbel, or Weibull) better fits the data sets, the R-squared (R^2) between the models and data sets for the cases $\xi \neq 0$ and $\xi = 0$ (see Equations 2 and 3, respectively) were computed. The shape parameter (ξ) of the GEV distribution was estimated. Table 1 details the R^2 from the fitting, showing that the Fréchet distribution ($\xi \neq 0$) is appropriate for v, N, and T, while the Gumbel distribution ($\xi = 0$) is appropriate for B and E.

Figure 2 shows the results, from top to bottom row, of the extreme event analysis of the interplanetary magnetic field magnitude, solar proton speed, solar proton density, solar proton temperature, and solar wind electric field, vB_z. The left column (panels a–e) shows the return plots obtained from the extreme event analysis and also the estimated values for 1-in-40 and 1-in-80 years marked with red crosses, while the right column shows (panels f–j) the linear fit with use of the special coordinate $-\log(-\log(p))$ against the logarithm of the magnitude for solar proton speed (panel g), solar proton density (panel h), solar proton temperature (panel i), against the magnitude for the interplanetary magnetic field (panel f), and solar wind electric field (panel j). This distinction is based on the distribution function used, Fréchet or Gumbel. The largest values are represented by the blue dots, while the orange dashed line is the linear fit. The orange straight lines are the 99% confidence intervals.

On some of these plots, dots are grouped in clusters as it is seen in Figure 2a or Figure 2c for the interplanetary magnetic field or the solar proton density. Every space weather event on these plots is represented by a single point, and the clusters show that perturbations of the solar wind parameters during strong space weather events can be significantly larger than during moderate activity. Thus, the cluster of the 10 largest B values in Figures 2a and 2f demonstrates that during very rare and severe space weather events the magnetic field achieves values between 56 and 80 nT (e.g., 60 nT on 29 October 2003, the Halloween storm), but all other perturbations of the magnetic field do not exceed 44.5 nT.

Table 2 details the results from the extreme event analysis such as the thresholds (Th) above which we will consider extreme events, and the estimated return values for 1-in-40 (Xtr_{40}) and 1-in-80 (Xtr_{80}) years.

The solar wind electric field, vB_z which is understood as a proxy of the response of the magnetosphere to the solar wind disturbances has been computed here as $E = v|B_z|$ for the negative values of B_z and is set to 0 for $B_z \geq 0$ because the response of the magnetosphere is strongly associated with the negative values of B_z (Gonzalez et al., 1994).

5. Discussion and Conclusions

In recent history, the dependence of modern society on technology has increased, and this rapid growth is expected to continue in the coming decades. Therefore, the study of potentially hazardous space weather events is crucial to mitigate the risks from these events to vulnerable technology.

This study provides an analysis of the extreme values of the solar wind characterized by the interplanetary magnetic field magnitude, solar proton speed, solar proton temperature, and solar proton density. Also, the extreme influence from space weather events to the magnetosphere was analyzed using the solar wind electric field, vB_z. The extreme value distribution was applied to the data set to estimate the magnitude of these characteristics for 1-in-40- and 1-in-80-year events to evaluate the largest possible risks from extreme disturbances in the solar wind.

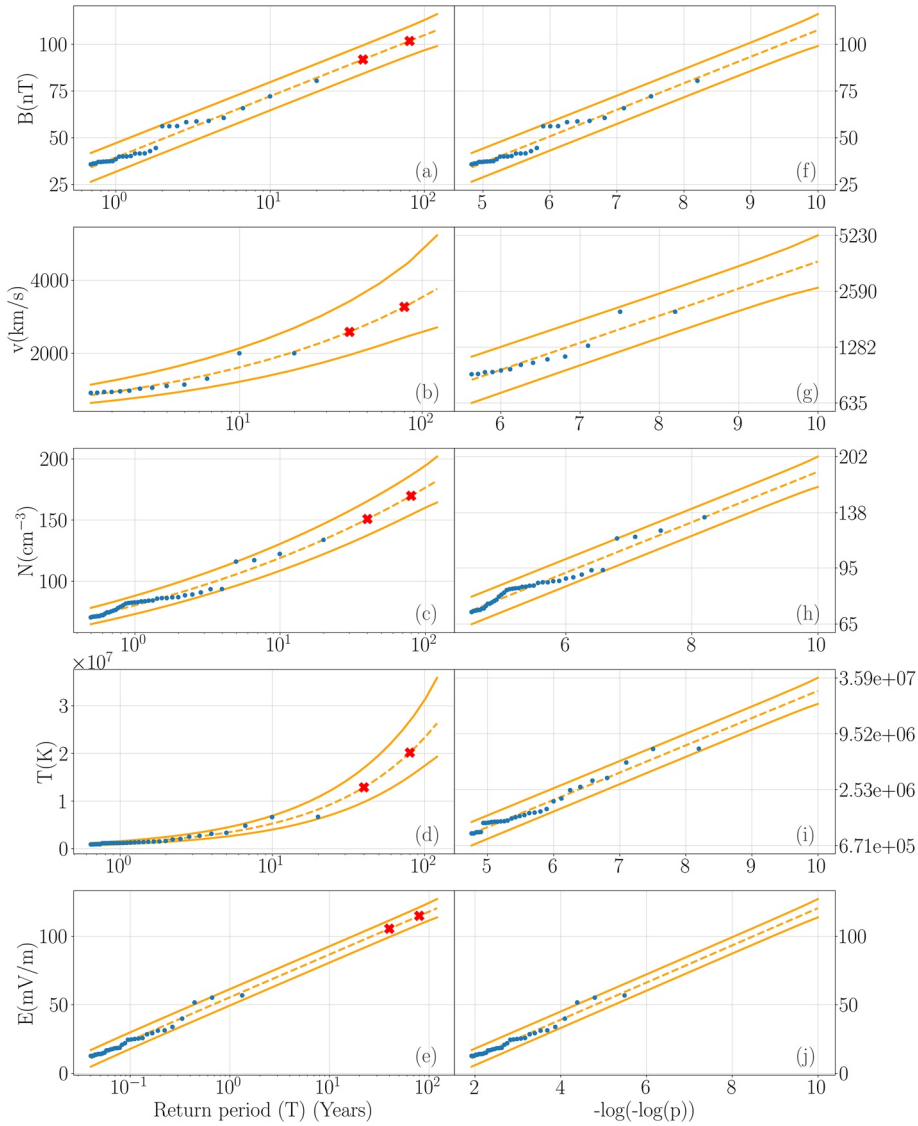

Figure 2. (Left column, panels from a to e) Estimation of extreme values for 1-in-40- and 1-in-80-year events (red crosses) with the 99% confidence interval (Right column, panels from f to j). Fitting block maxima to extreme value distributions. From top to bottom row, interplanetary magnetic field magnitude, solar proton speed, solar proton density, solar proton temperature, and solar wind electric field, vB_z.

The range of values obtained from the extreme value analysis of the solar wind magnitudes is in agreement with the empirical values described in previous studies. Cliver et al. (1990) analyzed severe geomagnetic storms from 1938 to 1989 and estimated a maximum speed of the solar wind at Earth, which is ~2,000 km/s. Skoug

Table 2
Threshold (Th) and Estimated Return Values for 1-in-40 (Xtr_{40}) and 1-in-80 years (Xtr_{80}) for Interplanetary Magnetic Field Magnitude (B), Solar Proton Speed (v), Solar Proton Density (N), Solar Proton Temperature (T), and Solar Wind Electric Field

	B (nT)	v (km/s)	N (cm^{-3})	T (10^7K)	E (mV/m)
Th	34	850	71	0.089	14
Xtr_{40}	92 (84–99)	2,582 (1,963–3,424)	151 (138–166)	1.3 (0.99–1.7)	69(63–75)
Xtr_{80}	102 (94–110)	3,270 (2,437–4,412)	170 (155–187)	2.0 (1.5–2.7)	79(72–85)

et al. (2004) estimated a speed at 1 AU ~2,000 km/s for the ICMEs of 29–30 October 2003. Liu et al. (2014) estimated a speed at 1 AU ~2,200 km/s for the ICME in July 2012, while Baker et al. (2013) estimated the speed to be ~2,500 km/s. The estimation from these researches of the extreme value of the speed agrees with the empirical results for the speed of ICMEs, since the obtained values are ~2,600 and ~3,200 km/s for the return period of 1-in-40 and 1-in-80 years. For the geomagnetic storm in August 1972, D'uston et al. (1977) measured values of the interplanetary magnetic field between 50 and more than 100 nT. Liu et al. (2020) suggest an upper boundary of ~100 nT. This range of values is compatible with our estimation of ~90 and ~100 nT for 1-in-40 and 1-in-80 years. Wilson et al. (2018) analyzed 10 years of data from the Wind spacecraft, estimated a maximum value for the solar proton temperature of $\sim 1 \cdot 10^7$ K, while the results show $1.3 \cdot 10^7$ K and $2.0 \cdot 10^7$ K for 1-in-40 and 1-in-80 years. Crooker et al. (2000) estimate that the highest density recorded is ~185 cm^{-3}, which agrees with ~150 and ~170 cm^{-3} as the return values for 1-in-40 and 1-in-80 years.

As it was discussed earlier, the sign of the shape parameter (ξ) defines the form of the GEV distribution. The results from the fitting procedure have shown that the confidence interval for the shape parameter in Table 1 covers negative values for some magnitudes, which is compatible with the Weibull distribution. This form of the GEV distribution is characterized by an upper boundary for the estimated return values. Therefore, these results suggest that these magnitudes could have an upper boundary. To narrow the confidence interval of the shape parameter to clarify this point, it is necessary to perform analyses with a time period longer than 20 years.

Data Availability Statement

The solar wind data set used in this research is publicly available and can be downloaded from the SWEPAM-SWICS/ACE (http://www.srl.caltech.edu/ACE/ASC/level2/lvl3DATA_SWEPAM-SWICS.html) and MAG/ACE (http://www.srl.caltech.edu/ACE/ASC/level2/lvl2DATA_MAG.html) webpages.

Acknowledgments
This work was supported by the MINECO project AYA2016-80881-P (including FEDER funds) and project PID2020-119407GB-I00/AEI/10.13039/501100011033. The authors would like to thank the Geomagnetic Laboratory of Natural Resources of Canada for making this collaboration possible and personally thank Dr. L. Trichtchenko, Dr. D. Boteler and Dr. R. Fiori for useful discussions. The authors want to thank the ACE Science Center for the coordination of different tools and resources available. More specifically, they thank the ACE SWEPAM, SWICS, and MAG teams for providing the data sets, downloaded from http://www.srl.caltech.edu/ACE/ASC/level2/lvl3DATA_SWEPAM-SWICS.html and http://www.srl.caltech.edu/ACE/ASC/level2/lvl2DATA_MAG.html.

References

Acero, F. J., Gallego, M. C., García, J. A., Usoskin, I. G., & Vaquero, J. M. (2018). Extreme value theory applied to the millennial sunspot number series. *The Astrophysical Journal*, *853*(1), 80. https://doi.org/10.3847/1538-4357/aaa406

Asensio Ramos, A. (2018). Extreme value theory and the solar cycle. *Astronomy & Astrophysics*, *472*(1), 293–298. https://doi.org/10.1051/0004-6361:20077574

Baker, D. N., Li, X., Pulkkinen, A., Ngwira, C. M., Mays, M. L., Galvin, A. B., & Simunac, K. D. C. (2013). A major solar eruptive event in July 2012: Defining extreme space weather scenarios. *Space Weather*, *11*(10), 585–591. https://doi.org/10.1002/swe.20097

Boteler, D. H. (2019). A 21st century view of the March 1989 magnetic storm. *Space Weather*, *17*(10), 1427–1441. https://doi.org/10.1029/2019SW002278

Chen, S., Chai, L., Xu, K., Wei, Y., Rong, Z., & Wan, W. (2019). Estimation of the occurrence probability of extreme geomagnetic storms by applying extreme value theory to aa index. *Journal of Geophysical Research: Space Physics*, *124*(12), 9943–9952. https://doi.org/10.1029/2019JA026947

Cliver, E. W., Feynman, J., & Garrett, H. B. (1990). An estimate of the maximum speed of the solar wind, 1938–1989. *Journal of Geophysical Research*, *95*(A10), 17103–17112. https://doi.org/10.1029/JA095iA10p17103

Coles, S. (2001). *An introduction to statistical modeling of extreme values* (1st ed.). Springer-Verlag London.

Crooker, N. U., Shodhan, S., Gosling, J. T., Simmerer, J., Lepping, R. P., Steinberg, J. T., & Kahler, S. W. (2000). Density extremes in the solar wind. *Geophysical Research Letters*, *27*(23), 3769–3772. https://doi.org/10.1029/2000GL003788

D'uston, C., Bosqued, J. M., Cambou, F., Temny, V. V., Zastenker, G. N., Vaisberg, O. L., & Eroshenko, E. G. (1977). Energetic properties of interplanetary plasma at the earth's orbit following the august 4, 1972 flare. *Solar Physics*, *51*(1), 217–229. https://doi.org/10.1007/BF00240459

Elvidge, S. (2020). Estimating the occurrence of geomagnetic activity using the Hilbert-Huang transform and extreme value theory. *Space Weather*, *18*(8), e02513. https://doi.org/10.1029/2020SW002513

Embrechts, P., & Schmidli, H. (1994). Modelling of extremal events in insurance and finance. *Zeitschrift für Operations Research*, *39*(1), 1–34. https://doi.org/10.1007/BF01440733

Gloeckler, G., Cain, J., Ipavich, F. M., Tums, E. O., Bedini, P., Fisk, L. A., et al. (1998). Investigation of the composition of solar and interstellar matter using solar wind and pickup ion measurements with SWICS and SWIMS on the ACE spacecraft. *Space Science Reviews*, *86*(1), 497–539. https://doi.org/10.1023/A:1005036131689

Gonzalez, W. D., Joselyn, J. A., Kamide, Y., Kroehl, H. W., Rostoker, G., Tsurutani, B. T., & Vasyliunas, V. M. (1994). What is a geomagnetic storm? *Journal of Geophysical Research*, *99*(A4), 5771–5792. https://doi.org/10.1029/93JA02867

Gopalswamy, N. (2016). History and development of coronal mass ejections as a key player in solar terrestrial relationship. *Geoscience Letters*, *3*(1), 8. https://doi.org/10.1186/s40562-016-0039-2

Gumbel, E. J. (1958). *Statistics of extremes*. Columbia University Press. https://doi.org/10.7312/gumb92958

Koons, H. C. (2001). Statistical analysis of extreme values in space science. *Journal of Geophysical Research*, *106*(A6), 10915–10921. https://doi.org/10.1029/2000JA000234

Liu, Y. D., Chen, C., & Zhao, X. (2020). Characteristics and importance of "ICME-in-sheath" phenomenon and upper limit for geomagnetic storm activity. *The Astrophysical Journal Letters*, *897*(1), L11. https://doi.org/10.3847/2041-8213/ab9d25

Liu, Y. D., Luhmann, J. G., Kajdič, P., Kilpua, E. K. J., Lugaz, N., Nitta, N. V., et al. (2014). Observations of an extreme storm in interplanetary space caused by successive coronal mass ejections. *Nature Communications*, *5*, 3481. https://doi.org/10.1038/ncomms4481

Love, J. J. (2019). Some experiments in extreme-value statistical modeling of magnetic superstorm intensities. *Space Weather*, *18*(1). https://doi.org/10.1029/2019SW002255

Love, J. J., Rigler, E. J., Pulkkinen, A., & Riley, P. (2015). On the lognormality of historical magnetic storm intensity statistics: Implications for extreme-event probabilities. *Geophysical Research Letters*, *42*(16), 6544–6553. https://doi.org/10.1002/2015GL064842

McComas, D. J., Bame, S. J., Barker, P., Feldman, W. C., Phillips, J. L., Riley, P., & Griffee, J. W. (1998). Solar Wind Electron Proton Alpha Monitor (SWEPAM) for the Advanced Composition Explorer. *Space Science Reviews*, *86*, 563–612. https://doi.org/10.1023/A:1005040232597

Nikitina, L., Trichtchenko, L., & Boteler, D. H. (2016). Assessment of extreme values in geomagnetic and geoelectric field variations for Canada. *Space Weather*, *14*(7), 481–494. https://doi.org/10.1002/2016SW001386

O'Brien, T. P., Fennell, J. F., Roeder, J. L., & Reeves, G. D. (2007). Extreme electron fluxes in the outer zone. *Space Weather*, *5*(1), 01001. https://doi.org/10.1029/2006SW000240

Riley, P., Baker, D., Liu, Y. D., Verronen, P., Singer, H., & Güdel, M. (2018). Extreme space weather events: From cradle to grave. *Space Science Reviews*, *214*, 21. https://doi.org/10.1007/s11214-017-0456-3

Ruzmaikin, A., Feynman, J., & Stoev, S. A. (2011). Distribution and clustering of fast coronal mass ejections. *Journal of Geophysical Research*, *116*(A4), A04220. https://doi.org/10.1029/2010JA016247

Siscoe, G. L. (1976). On the statistics of the largest geomagnetic storms per solar cycle. *Journal of Geophysical Research*, *81*(25), 4782–4784. https://doi.org/10.1029/JA081i025p04782

Skoug, R. M., Gosling, J. T., Steinberg, J. T., McComas, D. J., Smith, C. W., Ness, N. F., & Burlaga, L. F. (2004). Extremely high speed solar wind: 29–30 October 2003. *Journal of Geophysical Research*, *109*(A9), A09102. https://doi.org/10.1029/2004JA010494

Smith, C. W., L'Heureux, J., Ness, N. F., Acuña, M. H., Burlaga, L. F., & Scheifele, J. (1998). The ACE magnetic fields experiment. *Space Science Reviews*, *86*, 613–632. https://doi.org/10.1023/A:1005092216668

Thomas, M., Lemaitre, M., Wilson, M. L., Viboud, C., Yordanov, Y., Wackernagel, H., & Carrat, F. (2016). Applications of extreme value theory in public health. *PLoS One*, *11*, 1–7. https://doi.org/10.1371/journal.pone.0159312

Thomson, A. W. P., Dawson, E. B., & Reay, S. J. (2011). Quantifying extreme behavior in geomagnetic activity. *Space Weather*, *9*(10), S10001. https://doi.org/10.1029/2011SW000696

Trichtchenko, L. (2021). Frequency considerations in GIC applications. *Space Weather*, *19*(8). https://doi.org/10.1029/2020SW002694

Wilson, I. I. I., Lynn, B., Stevens, M. L., Kasper, J. C., Klein, K. G., Maruca, B. A., et al. (2018). The statistical properties of solar wind temperature parameters near 1 AU. *The Astrophysical Journal*, *236*, 41. https://doi.org/10.3847/1538-4365/aab71c

Zhang, J., Poomvises, W., & Richardson, I. G. (2008). Sizes and relative geoeffectiveness of interplanetary coronal mass ejections and the preceding shock sheaths during intense storms in 1996–2005. *Geophysical Research Letters*, *35*(2). https://doi.org/10.1029/2007GL032045